

# **Effect of Transition Taper Length on Air-Filled Substrate Integrated Waveguide Losses**

By:

**IBRAHIM MAHAMAT YASSINE MAHAMAT**

(MATRIX NO.: 140703)

SUPERVISOR:

**Dr. Nur Hidayah Binti Mansor**

July 2022

This dissertation is submitted to  
Universiti Sains Malaysia  
As partial fulfilment of the requirement to graduate with honours degree in  
**BACHELOR OF ENGINEERING (MECHANICAL ENGINEERING)**



School of Mechanical Engineering  
Engineering Campus  
Universiti Sains Malaysia

## Declaration

This work has not previously been accepted in substance for any degree and is not being concurrently submitted in candidature for any degree.

Signed.......... (IBRAHIM MAHAMAT YASSINE MAHAMAT)

Date..... 24/07/2022 .....

## STATEMENT 1

This thesis is the result of my own investigations, except where otherwise stated.

Other sources are acknowledged by giving explicit references.


Bibliography/references are appended.

Signed.......... (IBRAHIM MAHAMAT YASSINE MAHAMAT)

Date..... 24/07/2022 .....

## STATEMENT 2

I hereby give consent for my thesis, if accepted, to be available for photocopying and for interlibrary loan, and for the title and summary to be made available outside organisations.

Signed.......... (IBRAHIM MAHAMAT YASSINE MAHAMAT)

Date..... 24/07/2022 .....

## **Acknowledgement**

First and foremost, I would like to express my deepest gratitude to my dedicated supervisor, Dr. Nur Hidayah Binti Mansor for guidance, supervision, suggestion, and advice rendered throughout this work.

I must express my gratitude to my beloved parents, brothers, and sisters for their unlimited support, sincere concern, and endless encouragement and love throughout my study. Special thanks to all my beloved friends, colleagues, seniors and juniors for their unselfish help, kindness, motivation, and moral support. Thank you all!

## Table of Content

<b>Declaration</b> .....	<b>II</b>
<b>Acknowledgement</b> .....	<b>III</b>
<b>Table of Content</b> .....	<b>IV</b>
<b>List of Table</b> .....	<b>V</b>
<b>List of Figures</b> .....	<b>V</b>
<b>LIST OF ABBREVIATIONS</b> .....	<b>VI</b>
<b>Abstract</b> .....	<b>VII</b>
<b>Abstrak</b> .....	<b>1</b>
<b>CHAPTER 1 INTRODUCTION</b> .....	<b>1</b>
1.1    A brief overview of the overall structure of the project .....	1
1.2    Problem Statement.....	3
1.3    Objectives .....	4
1.4    Scope of Project.....	4
<b>CHAPTER 2 LITERATURE REVIEW</b> .....	<b>5</b>
2.1    Introduction .....	5
2.2    Substrate Integrated Waveguide (SIW).....	6
2.3    Air-filled Substrate Integrated Waveguide (AFSIW).....	9
2.4    TRANSITION FROM AIR TO DIELECTRIC-FILLED SIW .....	10
2.5    TRANSITION FROM DIELECTRIC-FILLED TO AIR-FILLED SIW.....	11
2.6    Effect of the Transition Length .....	12
<b>CHAPTER 3 METHODOLOGY</b> .....	<b>16</b>
3.1    Introduction .....	16
3.2    Flow chart for the design process.....	16
3.3    Numerical results for Air filled SIW .....	17
3.4    Simulation.....	19
3.5    Ansys HFSS.....	20
3.6    Design steps.....	21
<b>CHAPTER 4 RESULTS AND DISCUSSIONS</b> .....	<b>29</b>
4.1    Introduction .....	29
4.2    Simulation Results and Discussion .....	29
4.3    Regression graphs.....	33
<b>CHAPTER 5 CONCLUSION AND FUTURE WORK</b> .....	<b>35</b>
5.1    Conclusion.....	35
5.2    Future work .....	35
<b>Reference</b> .....	<b>37</b>
<b>Appendix</b> .....	<b>41</b>

## List of Table

Table 2.1 EQUATIONS FOR TAPER.....	12
Table 3.1 Structural properties of SIW.....	19
Table 4.1 shows a comparison of the V- and W-bands.....	32

## List of Figures

Figure 1.1 Sketch of a substrate integrated waveguide (SIW)[1].....	1
Figure 1.2 (a) SIW and (b) AFSIW cross-sectional views. [4] .....	2
Figure 1.3 Comparison of standard transmission line, RWG, SIW and AFSIW properties.[4].....	3
Figure 2.1 Substrate integrated waveguide and the equivalent rectangular waveguide.[13] .....	6
Figure 2.2 a) Sketch of a SIW. b) Periodic cell of SIW. c) Enclosed periodic cell. [16].....	7
Figure 2.3 Diagram of via holes with the surface impedance concept [17] .....	8
Figure 2.4 Air-filled SIW (a) cross sectional view and (b) Structure[18].....	9
Figure 2.5 Geometry of the proposed tapered transition with cross-sectional views [21] .....	11
Figure 2.6 Equation functions of taper. ....	12
Figure 2.7 Simulated S11 (left) and S21 (right) in Ka-band.[21].....	13
Figure 2.8 Simulated S11 (left) and S21 (right) in U-band.[21] .....	13
Figure 2.9 The reflection coefficient $ S_{11} $ vs ten different transition lengths[5] .....	14
Figure 2.10 The reflection coefficient $ S_{21} $ vs ten different transition lengths[5] .....	14
Figure 3.1 Flow chart of the process design[5] .....	16
Figure 3.2 3D views of the AFSIW with direct copper and metallised via arrays. ....	17
Figure 3.3 Cross-sectional views of the AFSIW structure. ....	17
Figure 3.4 Tapered transition with cross-section[18]. ....	18
Figure 3.5 Design procedure.....	20
Figure 3.6 Screenshot of Ansys HFSS Electronics Desktop. ....	21
Figure 3.7 property design and the first substrate.....	21
Figure 3.8 2 <sup>nd</sup> substrate with a tapered shape .....	22
Figure 3.9 2 <sup>nd</sup> substrate with tapered shape and properties .....	22
Figure 3.10 2 <sup>nd</sup> substrate with a rectangular hole .....	23
Figure 3.11 A copper plate and its properties.....	23
Figure 3.12 3D design of the AFSIW .....	24
Figure 3.13 box and the characteristics of the box .....	24
Figure 3.14 assigning a boundary for the box .....	25
Figure 3.15 assigning boundary for the object .....	25
Figure 3.16 Port Area .....	26
Figure 3.17 Assigning excitation (wave port) .....	26
Figure 3.18 Wave port one properties .....	27
Figure 3.19 Wave port two properties .....	27
Figure 3.20 Driven solution configuration .....	28
Figure 4.1 Simulated S11 for different transition lengths in V-band .....	29
Figure 4.2 Simulated S21 for different transition lengths in V-band .....	30
Figure 4.3 Simulated S11 for different transition lengths in W-band .....	30
Figure 4.4 Simulated S21 for different transition lengths in W-band .....	31
Figure 4.5 V-band linear regression graph at various lengths .....	33
Figure 4.6 W-band linear regression graph at various lengths .....	34

## LIST OF ABBREVIATIONS

SIW	Substrate Integrated Waveguide
SIC	Substrate Integrated Circuit
RF	Radio Frequency
AFSIW	Air-Filled Substrate Integrated Waveguide
DFSIW	Dielectric Filled Substrate Integrated Waveguide
PCB	Printed Circuit Board
HFSS	High-Frequency Structure Simulator
MIC	Microwave Integrated Circuit
RWG	Rectangular waveguide
BI-RME	Boundary Integral Resonant Mode Expansion
GHz	Gigahertz
TE	Transverse Electric
TEM	Transverse electromagnetic
FR	Flame Retardant
dB	Decibels
FEM	Finite Element Method
FDTD	Finite-Difference Time-Domain
FIT	Finite Integration Technique
CST	Computer Simulation Technology
EM	Electromagnetic
WR	Waveguide Rectangular

## Abstract

The SIW structure has been enhanced by using air as the propagation medium in order to reduce losses and increase its power-handling capacity. This transition connects dielectric structures to air structures. Improving SIW performance requires the development of a low-loss dielectric-to-air transition.

Using the Ansys HFSS software, this research will investigate the effects of transition taper length on air-filled substrate Integrated Waveguide Losses as well as how regression can be used to look at the link between length and losses.

To further decrease transition losses, the linear spline function is used to determine the transition taper's shape. The width of the dielectric filled SIW is  $W$ , whereas the width of the air-filled SIW is  $W_2$ , and the total width of the air-filled component is  $W_1$ . For the period of the transition,  $L$ , the width of the taper,  $W_2$ , rises while the widths of the transition taper,  $a$  and  $b$ , stay constant. The transitions exhibit the following structural characteristics:  $L$  is 30 millimetres and  $h$  is 0.508mm. Utilize the four fixed values of 30, 25, 20, and 15 mm to produce a set of curves that characterise the form of the taper in the simulation. In general, a transition length of 30 mm is deemed to result in acceptable losses. At the V-band and W-band frequencies, the  $\epsilon_r$  on the Roger RT/Duroid 6002 substrate switches from dielectric to air-filled SIW.

When the transition length is 15 millimetres, v-band return loss is greater than w-band return loss. The V-band has a lower return loss than the w-band at a 20 mm transition length, and the 25- and 30-mm return losses are similar.

This study shows how to reduce transition duration while retaining signal quality. The data might be used to develop a smaller, better microwave device that can be worn.

## Abstrak

Struktur SIW telah dipertingkatkan dengan menggunakan udara sebagai medium perambatan untuk mengurangkan kerugian dan meningkatkan kapasiti pengendalian kuasanya. Peralihan ini menghubungkan struktur dielektrik kepada struktur udara. Meningkatkan prestasi SIW memerlukan pembangunan peralihan dielektrik-ke-udara kehilangan rendah.

Dengan menggunakan perisian Ansys HFSS, penyelidikan ini akan menyiasat kesan panjang tirus peralihan pada Kehilangan Pandu Gelombang Bersepadu substrat berisi udara serta bagaimana regresi boleh digunakan untuk melihat pautan antara panjang dan kerugian.

Untuk mengurangkan lagi kehilangan peralihan, fungsi spline linear digunakan untuk menentukan bentuk tirus peralihan. Lebar SIW terisi dielektrik ialah  $W$ , manakala lebar SIW terisi udara ialah  $W_2$ , dan jumlah lebar komponen terisi udara ialah  $W_1$ . Untuk tempoh peralihan,  $L$ , lebar tirus,  $W_2$ , meningkat manakala lebar tirus peralihan,  $a$  dan  $b$ , kekal malar. Peralihan mempamerkan ciri-ciri struktur berikut:  $L$  ialah 30 milimeter dan  $h$  ialah 0.508mm. Gunakan empat nilai tetap 30, 25, 20, dan 15 mm untuk menghasilkan satu set lengkung yang mencirikan bentuk tirus dalam simulasi. Secara amnya, panjang peralihan 30 mm dianggap mengakibatkan kerugian yang boleh diterima. Pada frekuensi V-band dan W-band,  $\epsilon_r$  pada substrat Roger RT/Duroid 6002 bertukar daripada dielektrik kepada SIW berisi udara.

Apabila panjang peralihan ialah 15 milimeter, kehilangan pulangan jalur  $v$  lebih besar daripada kehilangan pulangan jalur- $w$ . Jalur- $V$  mempunyai kehilangan pulangan yang lebih rendah daripada jalur- $w$  pada panjang peralihan 20 mm, dan kerugian pulangan 25- dan 30-mm adalah serupa.

Kajian ini menunjukkan cara untuk mengurangkan tempoh peralihan sambil mengekalkan kualiti isyarat. Data mungkin digunakan untuk membangunkan peranti gelombang mikro yang lebih kecil dan lebih baik yang boleh dipakai.

# CHAPTER 1

## INTRODUCTION

### 1.1 A brief overview of the overall structure of the project

Emerging millimetre wave systems for communications, radar, and sensing applications need developing high-performance, low-cost technology. A substrate integrated waveguide (SIW), a subset of the substrate integrated circuits (SICs) family, has gotten much interest in the last decade. It is a rectangular electromagnetic waveguide formed on a dielectric substrate by tightly arraying metallized posts or through holes that connect the substrate's top and bottom metal plates. By using through-hole procedures through fences for the post walls, the waveguide may be easily compacted for mass manufacturing at a reasonable cost. A SIW has been proven to have similar guided wave and mode characteristics to a rectangular waveguide with an equivalent guide wavelength. Figure 1.1 depicts the critical dimensions of a substrate-integrated waveguide. [1]

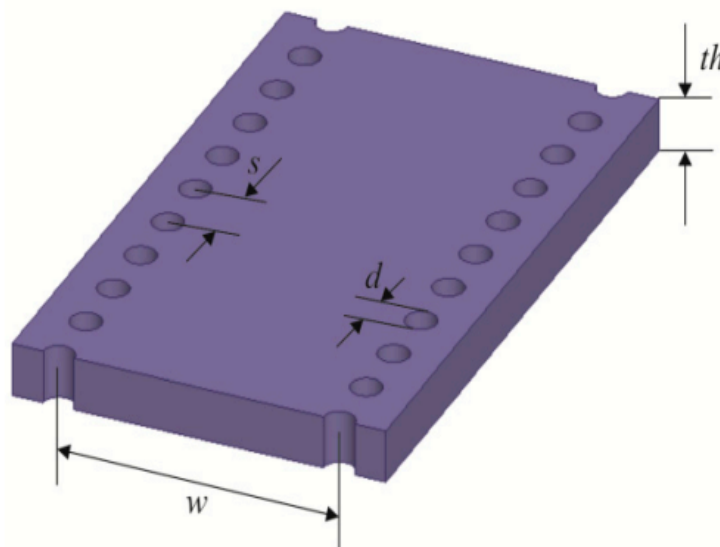


Figure 1.1 Sketch of a substrate integrated waveguide (SIW)[1]

SIW provides superior power handling capabilities, fewer radiation losses, cheaper manufacturing costs of different RF components utilising the SIW structure, and lower conductor loss due to the use of metal. Additionally, SIW has a lower loss of conductors due to the utilisation of metal. [2] Some of SIW's drawbacks are as follows: Significant leakage losses are caused by the spacing of holes placed on the top planes. Dielectric losses will arise

because dielectric is used in the waveguide construction rather than air in a conventional rectangular waveguide. Furthermore, since it is frequency dependent, mm-wave (millimetre wave) SIW applications must be thoroughly investigated. Because of its waveguide architecture, SIW has a lower cut-off frequency than other waveguide structures.[1]

In the early 2000s, Deslandes and Ke Wu came up with the concept of SIW to satisfy such requirements. They demonstrated a platform that could integrate all the components of a microwave circuit onto a single substrate with a rectangular area. Using a single substrate makes the volume and the simplicity of production more manageable. At the same time, the rectangular shape of the line's cross-section gives it the advantages of loss that come with waveguide construction. [3]

The SIW structure has been improved by using air as the propagation medium to decrease transmission and return losses and increase the ability to handle electricity. The transition is used to link dielectric structures to air structures. Improving SIW performance demands the creation of a dielectric-to-air transition with minimal loss.

Figure 1,2 shows the three-layer AFSIW design juxtaposed with the single-layer DFSIW architecture. AFSIW is a multilayer PCB composed of a top and bottom substrate (S1 and S3) that encompasses an inner substrate (S2). The centre layer comprises an air area with low dielectric loss and through side rows. Mechanical integrity preserves the dielectric slabs (width  $w$ ) on each side of the air area (width  $W$ ). The dielectric slabs do not influence losses since the E-field of the two basic TE<sub>10</sub> modes is confined in the low dielectric loss air area. [4]

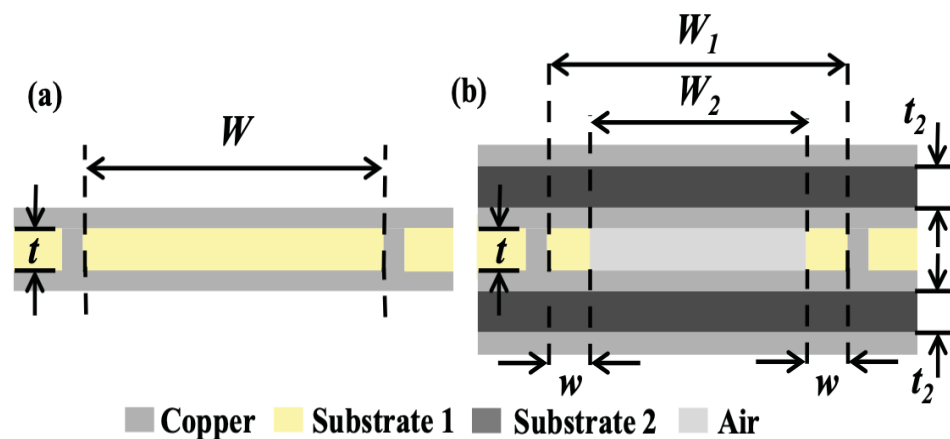


Figure 1.2 (a) SIW and (b) AFSIW cross-sectional views. [4]

The AFSIW is assembled via a technique involving many printed circuit boards layers. This up-and-coming technology has a cheap cost and an insertion loss equivalent to that of a

metallic waveguide with a small height. The metallic waveguide, the printed circuit board, the SIW, and the AFSIW are compared in figure 1.3 [4]

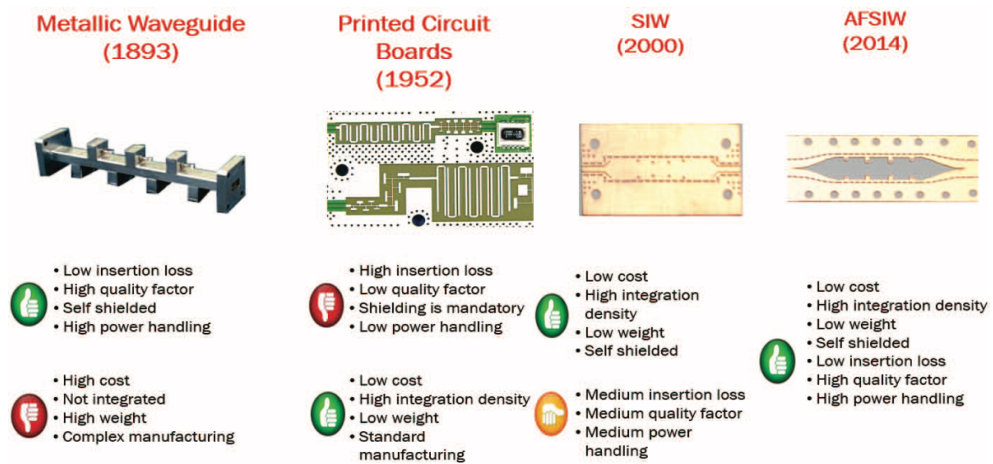


Figure 1.3 Comparison of standard transmission line, RWG, SIW and AFSIW properties.[4]

Within this project's context, HFSS software will be used to explore the impacts of Transition Taper Length on Air-Filled Substrate Integrated Waveguide Losses. The mathematical formulation and regression analysis of the link between length and losses is another primary emphasis of this endeavour.

## 1.2 Problem Statement

A more significant decrease in air-filled substrate integrated waveguide (AFSIW) losses at a shorter transition length is required for this project. This will enable a more compact design of printed substrate integrated waveguide (SIW) structures, resulting in the miniaturisation and enhanced performance of wearable microwave devices.[5]

Minimizing losses is the most challenging aspect of designing SIW components, mainly when they include signal transitions. Today, using air as the propagation medium to decrease losses and boost power handling capacity is a generally established strategy for enhancing SIW performance. [6]

Using SIW circuits in high-quality microwave and millimetre wave components may result in significant loss, which is one of the most significant drawbacks; compared to ohmic or radiation losses, dielectric loss is by far the leading cause of loss in SIW [5], [7]. As a result, this study will investigate the effect of transition taper length on AFSIW structure loss.

### 1.3 Objectives

There are three main objectives of this study:

- i. To do a full-wave analysis of the dielectric-to air-filled substrate integrated waveguide transition.
- ii. To evaluate the effects of the linear spline transition taper length on reflection and transmission losses in an air-filled SIW.
- iii. To study the relationship between length and losses.

### 1.4 Scope of Project

Using HFSS software, this project will investigate the effect of transition taper length on air-filled substrate Integrated Waveguide Losses. The project also looks at how the relationship between length and loss can be expressed mathematically and analysed using regression.

## CHAPTER 2

### LITERATURE REVIEW

#### 2.1 Introduction

This chapter discusses previous research on slotted waveguide antennas, substrate integrated waveguides, substrate integrated waveguide antennas, and transitions between microwave transmission lines and substrate integrated waveguides and air-filled substrate integrated waveguides.

The advantages of conventional waveguides, the first generation of microwave guiding structures, were a high-power carrying capacity and a high Q-factor, but their size was negative. The subsequent generation of microwave guiding elements consisted of the strip-like or slot-like planar printed transmission lines used in Microwave Integrated Circuits (MICs). These planar, low-profile structures lacked the standard waveguide's great power carrying capacity and high Q-factor. To bridge the gap between MIC structures and traditional waveguides, Substrate Integrated Circuits (SICs) were designed as planar, low-profile structures with high power carrying capacity and high Q-factor, similar to MIC structures [8].

Artificial channels were constructed within the substrate in order to direct the waves. These channels are built using two different methods (which are embedded in the substrate). Using metallic vias as sidewalls are one option. Total internal reflection may be facilitated by using contrast in the  $\epsilon_r$  values, which results in a restricted wave [9]

A SIW is one of the ways that SIC can be set up. SIW technology has made active circuits, passive components, antennas, and other microwave and millimetre-wave parts [10].

Deslandes, Wu, Jain, and Kinayman have shown that the idea can be used for microstrip transitions. Deslandes and Wu, as well as Ito et al., have also made coplanar waveguide transitions. Ito et al. and Tzuang et al. have shown how to make a simple waveguide filter. Also, no one knew how much radiation was lost through the gaps between the vias [11]. When a rectangular waveguide is added to a microstrip substrate, the Q-factor of the waveguide goes down because of dielectric filling and a decrease in volume [12]. Because SIW is similar to a typical rectangular waveguide filled with dielectric, it may be analysed using just the width of the analogous waveguide [13]. An experiment formula calculates the width of equivalent RWG. Figure 2.1 shows the physical parameter required in the equivalent rectangular waveguide

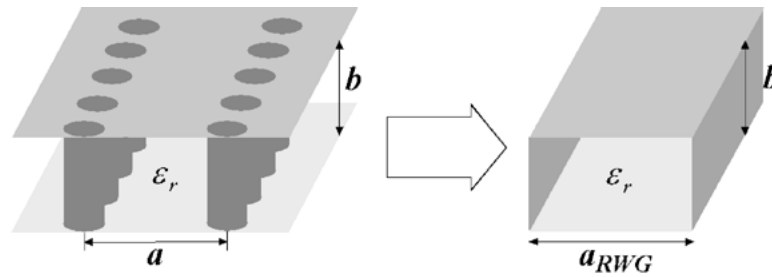


Figure 2.1 Substrate integrated waveguide and the equivalent rectangular waveguide.[13]

The integrated rectangular waveguide idea was recently put out. A synthetic waveguide is built using a linear array of posts or via-holes metalized and implanted in the same substrate as the planar circuit. Completely metallized walls may also be used to construct this waveguide. The waveguide may be excited by several transitions. In each of these designs, the rectangular waveguide, and planar circuits, such as microstrip lines or coplanar waveguides, are fabricated on the same substrate, and the transition between the two is created using a straightforward matching geometry. The synthetic integrated waveguide seems to be a suitable compromise between the air-filled rectangular waveguide and planar circuit based on its electrical performance [14].

## 2.2 Substrate Integrated Waveguide (SIW)

Several scholars have recently advocated SIW, a novel kind of transmission line. Commercially available components for different standard waveguide bands from 1 GHz to over 220 GHz include couplers, detectors, isolators, attenuators, and slot lines. The majority of microwave circuitry is presently produced using planar transmission lines like microstrip transition, coplanar transition, and others as a result of these trends towards miniaturisation and integration. High power systems, millimetre wave systems, and very accurate test systems are just a few applications that call for waveguides.[15]

Using the BI-RME approach and Floquet's theorem, Cassiviet examined substrate integrated waveguides (SIWs) to ascertain their dispersion properties [16]. The substrate of the SIW is coated with a thin metallic layer on the top and bottom, and metallic via holes are employed to mimic the side walls of a rectangular waveguide.

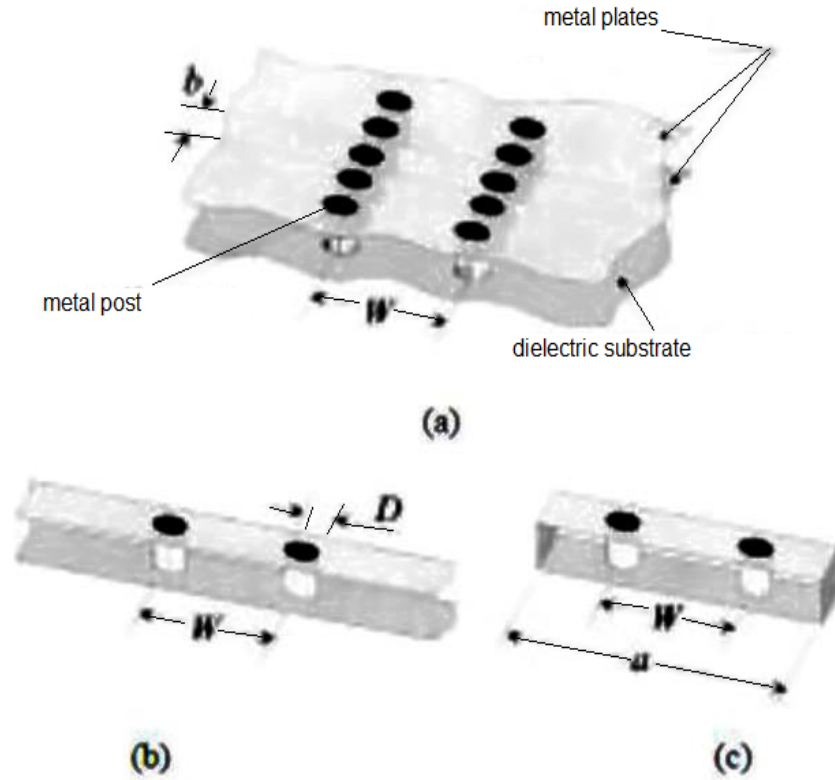


Figure 2.2 a) Sketch of a SIW. b) Periodic cell of SIW. c) Enclosed periodic cell. [16]

Figure 2.2 depicts an image of a SIW and a periodic cell of a SIW. The SIW is a periodic structure. The BI-RME approach calculates a generalised admittance matrix of the periodic cell. Because the SIW is periodic, an eigenvalue system may be obtained using Floquet's theorem. The pattern of the modal fields is represented by the eigenvectors, while the eigenvalues provide the propagation constants of the TE modes propagating through the SIW. Their research has shown that rectangular and substrate integrated waveguides have the same fundamental guided wave properties. Their empirically obtained formulae estimate the cut-off frequencies of the SIW's first two dominant modes.

$$f_{c_{TE10}} = \frac{c_0}{2\sqrt{\epsilon_r}} \left( a - \frac{d^2}{0.95 \cdot s} \right) \quad \text{Equation 2.1}$$

And

$$f_{c_{TE20}} = \frac{c_0}{\sqrt{\epsilon_r}} \left( a - \frac{d^2}{1.1 \cdot s} - \frac{d^3}{6.6 \cdot s} \right) \quad \text{Equation 2.2}$$

Where (a) represents the SIW width, (d) represents the diameter of the via holes, (s) represents the spacing between adjacent via holes, and ( $c_0$ ) represents the speed of light.

By comparing equation 2.1 with the equation that specifies the cut-off frequency of the dominant mode of rectangular waveguides, Cassivi et al. has produced an equation that relates the width of a SIW to an equivalent width of a rectangular waveguide [16].

$$a_{RWG} = a - \frac{d^2}{0.95 \cdot s} \quad \text{Equation 2.3}$$

It is far more challenging to create a SIW than a conventional waveguide. Deslandes and Wu created a straightforward design technique for converting a SIW to an equivalent rectangular waveguide [17]. Use the available finite element software package. This allows the designer to build a system using a conventional waveguide and then utilise their method to find an equivalent SIW to replace the rectangular waveguide.

Deslandes and Wu have established a technique for calculating the complex propagation constant of a SIW by using the idea of surface impedance to describe the rows of conducting cylinders that serve as the SIW's sidewalls [17]. Transverse resonance and a technique of moments are used to solve the given model. One way to see a TE mode wave's electromagnetic field is to superimpose two waves at an angle of zero to the Z-axis, which is the direction of energy propagation [17]. The two rows of metallic disperse the TEM waves through holes at the cut-off frequency. Surface impedance  $Z_S$  may be used to indicate a row of via holes. The two rows of via holes are seen in Figure 2.3.

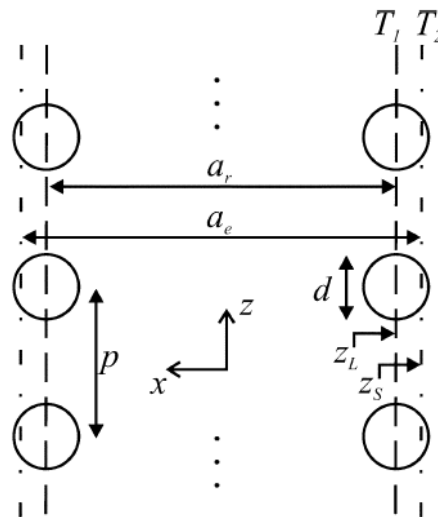


Figure 2.3 Diagram of via holes with the surface impedance concept [17]

A transverse resonance technique may compute the SIW's rectangular waveguide equivalent width ( $ae$ ). The reflection coefficient of the row of through holes at the desired cut-off frequency may be used to calculate the SIW propagation constant. Using the method of moments, the reflection coefficient of the through holes at the cut-off frequency may be computed. This approach is unusual in that the propagation constant of the SIW may be computed rapidly and precisely. This approach may also be utilised to extract the leakage characteristics of the periodic structure in addition to the guided-wave qualities of the SIW. Based on these findings, design principles have been proposed to limit leakage, prevent band gaps in the operational bandwidth, and help designers construct substrate-integrated waveguides. The first design criterion is simple: the separation distance ( $s$ ) must be greater than the diameter of the via hole ( $d$ ).

The second design rule says that the separation distance at the cut-off frequency must be less than a quarter wavelength. A third design criterion stipulates that the separation distance between the metallic cylinders should be less than  $2d$  to demonstrate minimum leakage loss. Promising experimental findings validated the hypothesis as mentioned above.

### 2.3 Air-filled Substrate Integrated Waveguide (AFSIW)

Figure 2.4 depicts the suggested architecture of Parment's AFSIW structure based on the multilayer PCB technology. Substrates 1 and 3 constitute the top and bottom conducting boundaries, respectively. They are positioned between the air-filled intermediate substrate and the metallic vias [18]. For manufacturing and mechanical integrity reasons, dielectric zones of width ( $w$ ) must remain on both sides of the waveguide. ( $w \geq 0.254$  mm for the PCB process at the Poly-Grames Research Centre). As the E-field of the basic  $TE_{10}$  mode is limited to the core of the waveguide, these dielectric slabs have a negligible effect on dielectric losses. For substrates 1 and 3, low-cost substrate material such as FR-4 may be utilised to construct baseband or digital circuitry to create a compact system.

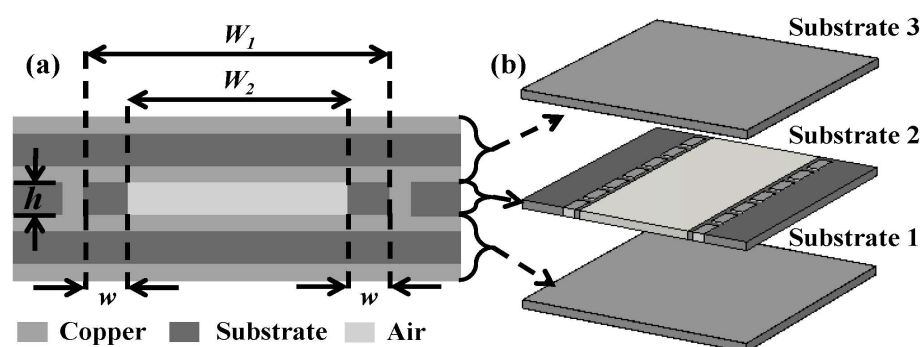


Figure 2.4 Air-filled SIW (a) cross sectional view and (b) Structure[18]

The cut-off frequency of a dielectric filled SIW is calculated using the following relationship[19]:

$$f_{c_{mn}} = \frac{c}{2\pi\sqrt{\epsilon_r}} \sqrt{\left(\frac{m\pi}{W}\right)^2 - \left(\frac{n\pi}{h}\right)^2} \quad \text{Equation 2.4}$$

where  $W$  and  $h$  are the width and height of SIW, respectively,  $m$  and  $n$  are the  $TE_{mn}$  mode indices,  $c$  is the velocity of light, and  $\epsilon_r$  is the permittivity of the substrate. As seen in Figure 2.4, the air-filled SIW is formed of two different dielectrics, hence equation 2.4 cannot be considered. Calculating the cut-off frequency of the fundamental  $TE_{10}$  mode requires consideration of the dielectric slabs on either side of the SIW. Using the Newton-Raphson technique of iteration to solve the characteristic equation, this cut-off frequency is determined in equation 2.5 [18], [20]:

$$\tan\left(\frac{\sqrt{\epsilon_r}(W_1-W_2)*\pi f_c}{c}\right) = \sqrt{\epsilon_r} \cot\left(\frac{W_2*\pi f_c}{c}\right) \quad \text{Equation 2.5}$$

$W_1$  and  $W_2$  are the air-filled SIW total width and the air-filled region width, respectively [21].

## 2.4 TRANSITION FROM AIR TO DIELECTRIC-FILLED SIW

Air-to-dielectric-filled SIW circuits may now be interconnected thanks to this article's transitional design proposal effectively. We are thinking: An air-filled substrate integrated waveguide (SIW) made from a multilayer printed circuit board technology is an appealing choice for millimetre-wave applications that need low cost, low loss, and efficient power management. In addition to lowering loss and increasing power handling capability, this air-filled, three-layered SIW is also very lightweight. An integrated millimetre-wave system may be made tiny by using low-cost common substrates like FR-4 for the top and bottom layers, which can then be used to build baseband or digital circuitry. An average of 0.168 dB/cm (0.098 dB/cm) is found in the air-filled SIW over the Ka-band (U band) compared to its dielectric-filled equivalents. The average power handling capability rises by 8 decibels (6 decibels), and the quality factor rises three times as much (3.0 decibels) [21].

Specifically, this technology is interested in millimetre-wave applications requiring low cost, low-loss performance, and power-handling solid capabilities. A wideband transition is suggested to interconnect the proposed air-filled SIW with the dielectric-filled SIW more easily. A back-to-back transition in the Ka-band is manufactured for validation reasons. In the

frequency range of 27-40 GHz, it achieves a return loss of better than 15 dB and an insertion loss of  $0.6 \pm 0.2$  dB ( $0.3 \pm 0.1$  dB for the transition) from 27 to 40 GHz.

The TE<sub>10</sub> dominant mode's cut-off frequency is kept practically constant during the transition in this study to prevent dispersions. Figure 5 depicts the intended transition. During the transition, the dimensions  $W_1$  and  $W_2$  grow in size. For each cross-section,  $W_1$  and  $W_2$  parameters are found using equation 2.5 to maintain a consistent cut-off frequency for all cross sections. [21] According to the paper, single-layer construction and usage in E and W bands are the main features of this shift. The high dielectric constant substrate is tapered from SIW to its low dielectric constant counterpart by a triangle-shaped high dielectric constant substrate. The transition is self-shielded because of its waveguide-based construction, and its noise interference is minimal [22]

The simulation optimises the distance between each discretized sector for a suitable return loss. Clearly, the better the transition performs, the more discretized points there are. For example, in [22], one dielectric substrate penetrates another dielectric substrate. Just the contrary is true [21]. Because the E-field of the TE<sub>10</sub> mode is focused on the centre of SIW, the lower loss material must penetrate the other to minimise dielectric losses during the transition [21]

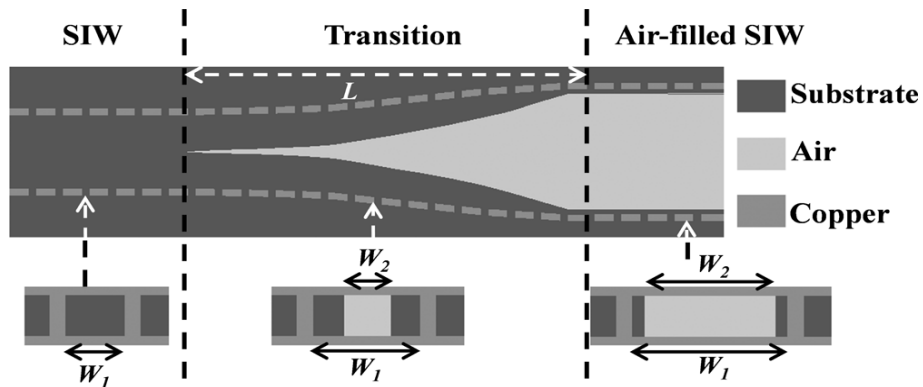


Figure 2.5 Geometry of the proposed tapered transition with cross-sectional views [21]

## 2.5 TRANSITION FROM DIELECTRIC-FILLED TO AIR-FILLED SIW

While the characteristic equation 2.5 governs the cut-off frequency, it also implies the effect of taper in the transition between dielectric filled SIW and air-filled SIW. The solution of equation 2.5 for  $W_1$  and  $W_2$  yields a constant  $f_c$  along the transition [23]. The taper design for the transition using the characteristic equation is effective in [18]. The transition from dielectric filled SIW to air-filled SIW is shown in Figure 2.5. The different functions of the

taper are shown in Figure 2.6. For the design of the taper, the width of the taper  $W(x)$  increases with the distance  $x$ , as shown in the taper equation in Table 2.1, where  $a$  and  $b$  are constants to ensure continuity of transition.

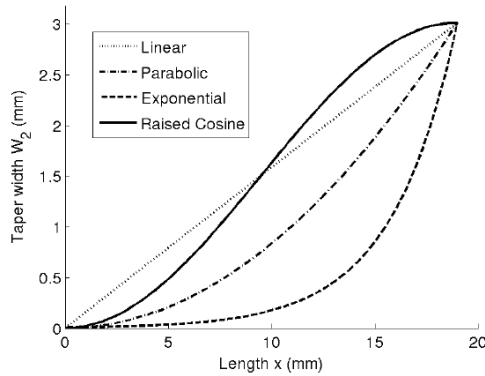


Figure 2.6 Equation functions of taper.

Table 2.1 EQUATIONS FOR TAPER

Shape	$W_2(x)$
Linear	$a + (b - a)(x/L)$
Parabolic	$a(b - a)(x/L)^2$
Exponential	$a + (b - a)\exp[5(x - L)/L]$
Raised cosine	$0.5(a + b) + 0.5(b - a)\cos[(x/L - 1)\pi]$

## 2.6 Effect of the Transition Length

The distance between cross sections in discretized sections acquired by equation 2.5 is imported into the simulation to maximise the transition duration without decreasing S-parameters. The research is carried out in the Ka and U bands on Rogers RT/Duroid 6002 for various lengths: 5-, 10-, 20-, and 30-mm. Figure 2.7 shows that the longer the transition, the better the matching. This conclusion may be drawn from figure 2.8. As a result, there is a trade-off between overall transition time and return loss. [21]

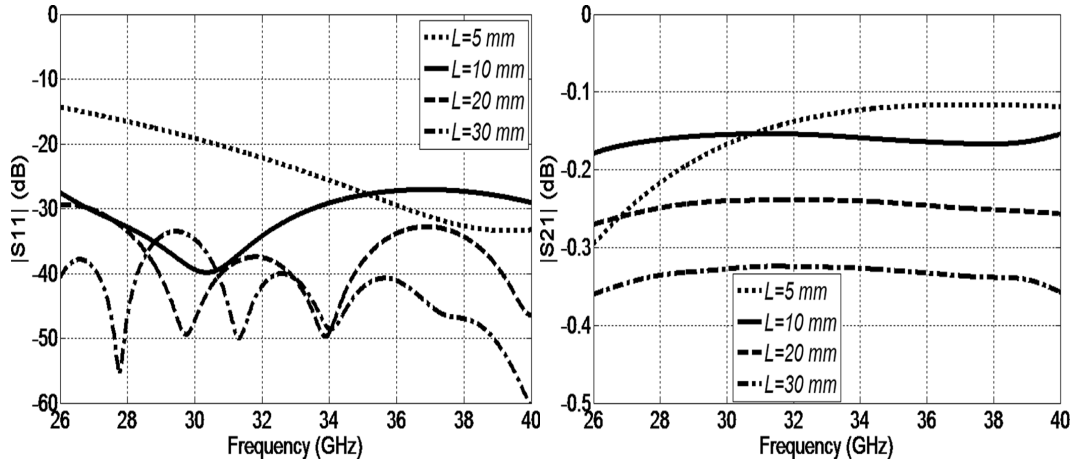


Figure 2.7 Simulated S11 (left) and S21 (right) in Ka-band.[21]

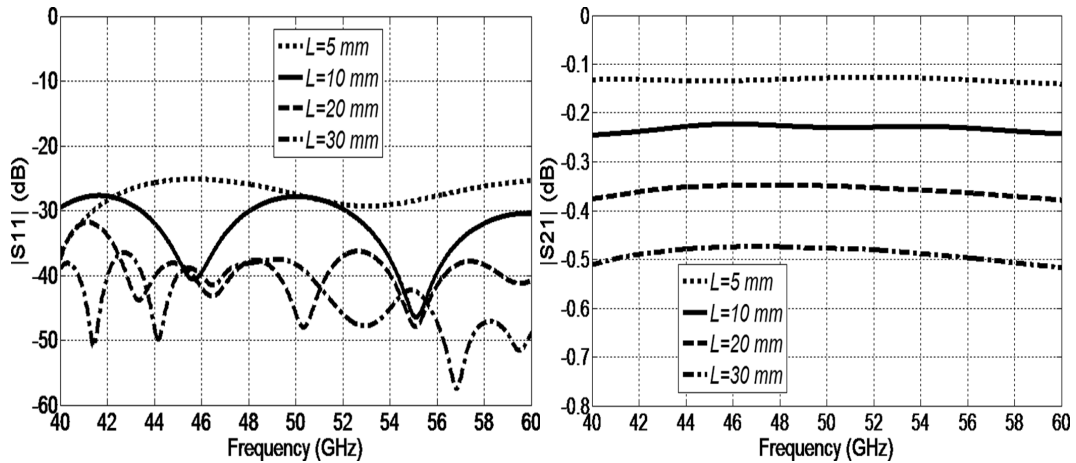


Figure 2.8 Simulated S11 (left) and S21 (right) in U-band.[21]

Figure 2.9 illustrates the result of the reflection coefficient  $S_{11}$  of 1 to 20 mm of transition length by a step size of 1 mm, according to Mansor H [5]. The  $S_{11}$  of the 1 to 3 mm transition length in Figure 2.9 (left) indicates that the air-filled SIW structure has a significant return loss. This incident wave is caused by the quick change between dielectric and air-filled waves and the way they do not match up [24].

As demonstrated in Figure 2.9, the  $S_{11}$  values decrease at specific frequencies. All figures show the link between resonant and transition length. According to Figure 9 (left), 33 GHz is a greater resonance frequency for a 4 mm transition length, but it becomes a lower

resonant frequency with a 7 mm transition length. As a result, increasing the length produces a shift in resonance frequency and a more than 20 dB increase in the return loss bandwidth. [5]

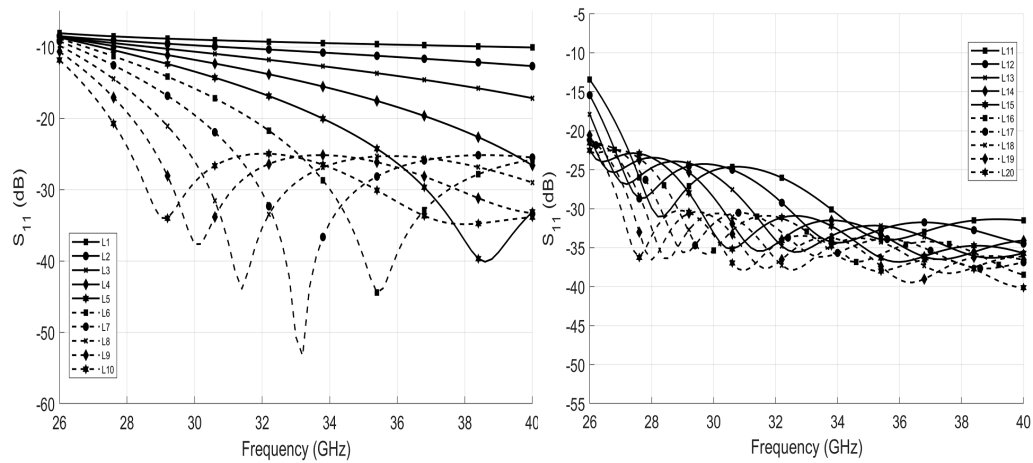


Figure 2.9 The reflection coefficient  $|S_{11}|$  vs ten different transition lengths[5]

As shown in Figure 2.10, the transmission loss rises gradually as the transition length extends from 11 to 20 mm due to resonance. Therefore, increasing the transition length results in a greater than 20 dB increase in the return loss bandwidth, suggesting that a broad bandwidth for the Ka-band may be attained by increasing the transition length. Sadly, this essentially increases the transition loss as well. Thus, bandwidth and transmission loss are in a relationship of trade-offs [5].

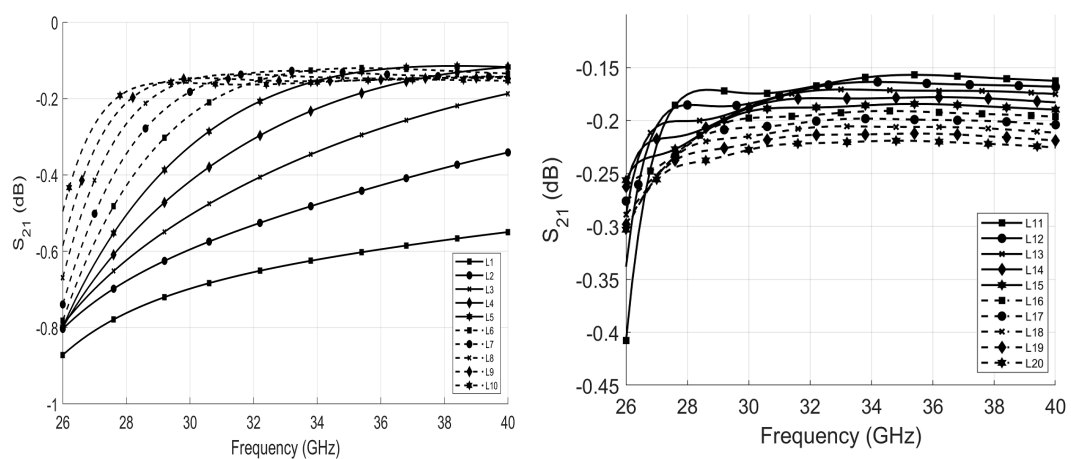


Figure 2.10 The reflection coefficient  $|S_{21}|$  vs ten different transition lengths[5]

AFSIW is a technology platform with minimal loss and low cost. It is a high-performance, low-cost alternative to the traditional rectangular waveguide. The multilayer PCB technique on which it is based allows for adjusting propagation mode properties, implementing conducting vias, and constructing compact multilayer components and circuits. There have been several publications of AFSIW passive devices in the literature. Developing active AFSIW devices is one of the phases toward developing a comprehensive system. The authors see AFSIW as a fundamental technology for upcoming millimetre communication and sensor systems [4].

## CHAPTER 3 METHODOLOGY

### 3.1 Introduction

First, this chapter will demonstrate the general process flowchart. After that, we will discuss the essential design equations for air-filled SIW, starting with how the E-field is spread out in the slot. An air-filled substrate integrated waveguide is designed by first changing the SIW into a rectangular waveguide.

Once the size (the width) of the corresponding rectangular waveguide has been determined, the following step is to build an air-filled SIW for a dielectric-filled waveguide with the previously determined width. Following an explanation of the HFSS simulator, this chapter will describe the design procedures. All the design approaches and theories established for the rectangular waveguide immediately apply.

### 3.2 Flow chart for the design process

Figure 3.1 shows the process of designing in general:

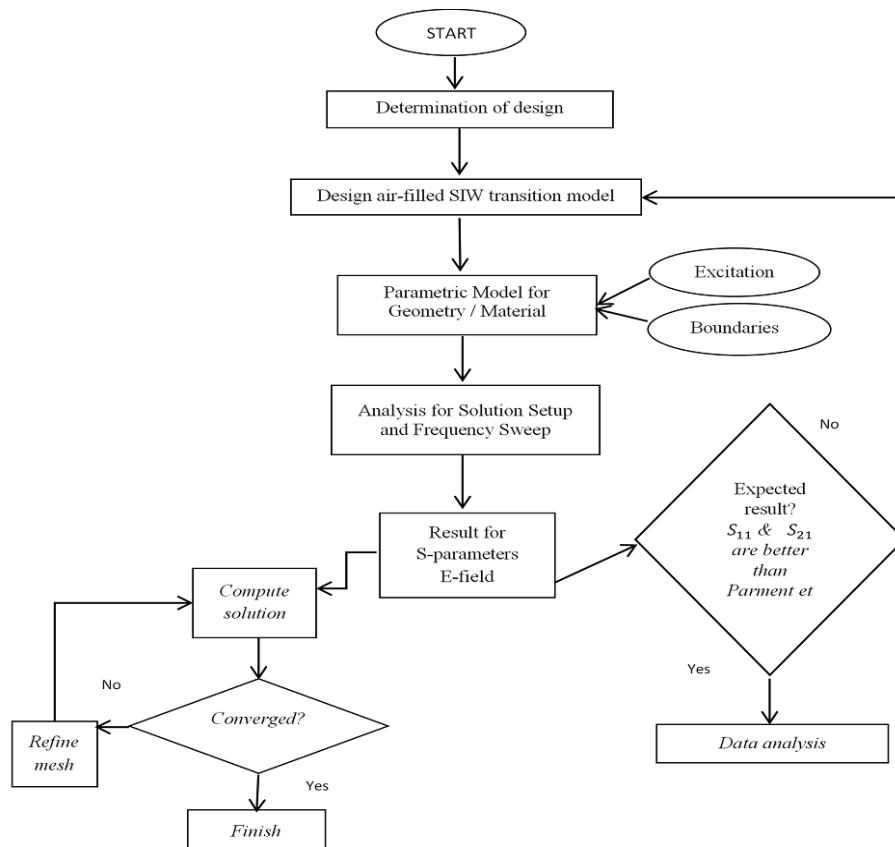


Figure 3.1 Flow chart of the process design[5]

### 3.3 Numerical results for Air filled SIW

The proposed AFSIW transmission line structure is illustrated in figures 3.2 and 3.3. It is based on the multilayer PCB process. Substrates 1 and 3, enclosing substrate 2, are used as bottom and top electrical walls of the AFSIW, respectively. Substrate 2 implements an air-filled propagation channel. The electric sidewalls of substrate two can be implemented with continuously metallized sidewalls or with arrays of metallized via, as represented in Figure 3.2 (a) and Figure 3.2 (b), respectively.

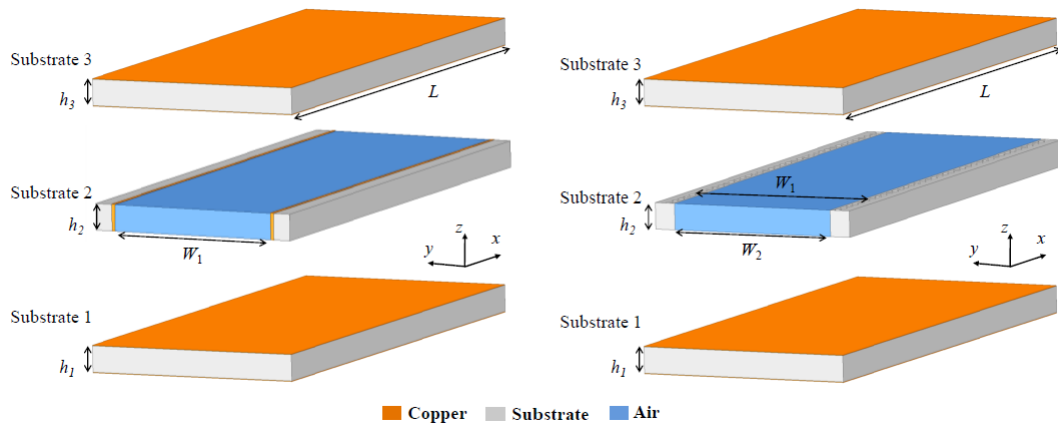


Figure 3.2 3D views of the AFSIW with direct copper and metallised via arrays.

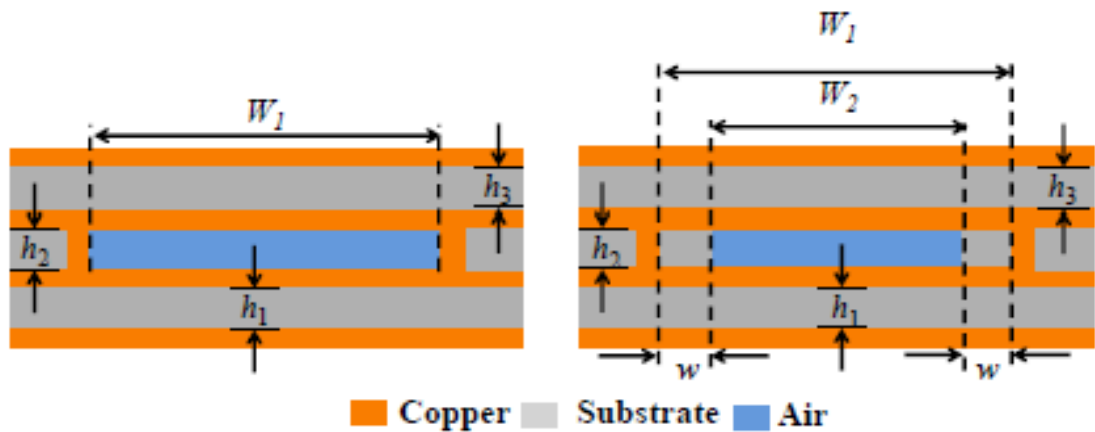


Figure 3.3 Cross-sectional views of the AFSIW structure.

Depending on the implementation of the electrical sidewalls of substrate 2, it is possible to determine the cut-off frequencies for the  $TE_{mn}$  mode. If the electric sidewalls are implemented with continuously metallized sidewalls, then the AFSIW structure is similar to an air-filled metallic rectangular waveguide of equal dimensions. Hence, the cut-off frequency for the  $TE_{mn}$  mode is given from the rectangular waveguide theory[18]:

$$f_{c_{mn}} = \frac{c}{2\pi\sqrt{\epsilon_r}} \sqrt{\left(\frac{m\pi}{W}\right)^2 + \left(\frac{n\pi}{h}\right)^2} \quad \text{Equation 3.1}$$

where  $W$  and  $h$  are the width and height of the SIW, respectively, and  $m$  and  $n$  are the indices of the  $TE_{mn}$  mode,  $c$  is the light velocity, and  $\epsilon_r$  is the dielectric constant.

As the air-filled SIW of Figure 4 is composed of two different dielectrics, Equation 3.1 provides only a fair approximation for small values of  $w$ . Otherwise, the dielectric slabs on each side of the SIW must be considered to determine the cut-off frequency of the fundamental  $TE_{10}$  mode. This cut-off frequency  $f_c$  is obtained using the Newton–Raphson method of iteration to solve the characteristic equation:

$$\tan\left(\frac{\sqrt{\epsilon_r}*(W_1-W_2)*\pi f_c}{c}\right) = \sqrt{\epsilon_r} \cot\left(\frac{W_2*\pi f_c}{c}\right) \quad \text{Equation 3.2}$$

Where  $W_1$  and  $W_2$  are the total width and the air-filled region width of the air-filled SIW, respectively.

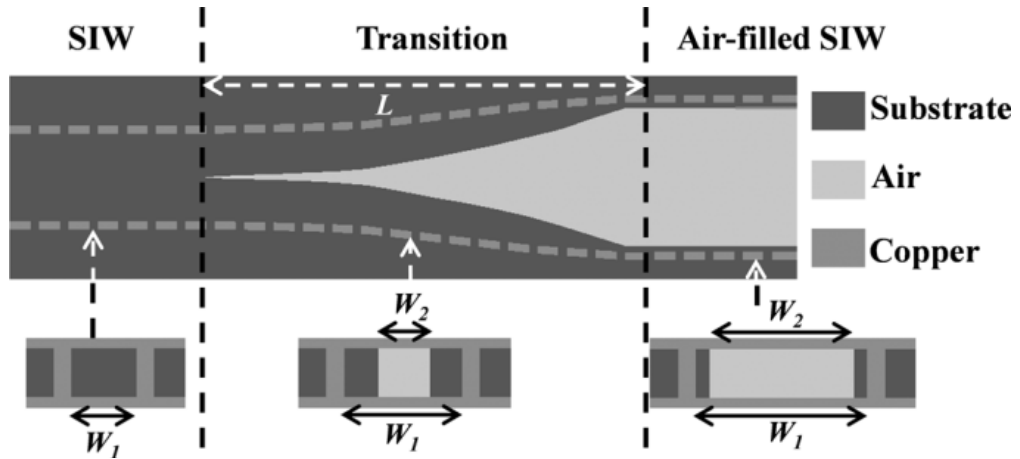


Figure 3.4 Tapered transition with cross-section[18].

In order to decrease transition losses, even more, the linear spline function is utilized to calculate the shape of the transition taper in figure 3.4.

The dielectric-filled SIW has a width of  $W$ , and the air-filled SIW has a width of  $W_2$ , with  $W_1$  being the total width of the air-filled portion.

As illustrated in figure 3.4, the width of the taper  $W_2$  increases throughout the transition length  $L$ . However, the widths  $a$  and  $b$  of the transition taper stay constant to ensure

the transition continues. Table 3.1 lists all of the structural characteristics of the transitions, where L is 20 mm, and h is 0.508 mm. As illustrated in Figure 3.4, in simulation, employ the four fixed values 20, 15, 10, and 5 to create a collection of curves that characterize the form of the taper. As stated in [21], a transition length of 20 mm is commonly accepted to provide acceptable losses. The dielectric to air-filled SIW transition is designed for the Roger RT/Duroid 6002 substrate  $\epsilon_r$  in the V-band and W-band frequencies.

Table 3.1 Structural properties of SIW

	Parameters (mm)	Dimension Properties	
		Air filled SIW	SIW
V-band	W1	3.7592	
	W2	2.7432	
	W		2.12
	$\epsilon_r$	2.94	2.94
	h	0.508	0.508
W-band	W1	2.54	
	W2	1.6	
	W		1.45
	$\epsilon_r$	2.94	2.94
	h	0.508	0.508

### 3.4 Simulation

Many 3D electromagnetic field models are widely utilised in both industry and academics. One of them is Ansoft HFSS. It calculates the electrical behaviour of high-frequency and high-speed components using a 3D full-wave Finite Element Method (FEM). While FIDELITY is an FDTD (Finite-Difference Time-Domain) based Full-3D EM Simulator,

and CST is based on the Finite Integration Technique (FIT), HFSS was the first commercial tool to simulate complicated 3D geometries. At the same time, CST is considered the industry standard development tool by many engineers. HFSS has been utilised for design and simulation purposes to aid this study.

This section presents simulations using the ANSYS HFSS electromagnetic (EM) programme. The proposed transmission is examined and tested in the WR-15 band's V-band satellite communication frequency range (50 to 75 GHz) and the WR-10 band's W-band satellite communication frequency range (75 to 110 GHz). This is because the AFSIW technical platform is intended to be valuable for space applications.

### 3.5 Ansys HFSS

Ansys HFSS is 3D electromagnetic (EM) simulation software for designing and testing high-frequency electronic devices such as antennas, antenna arrays, RF or microwave components, high-speed interconnects, filters, connectors, integrated circuit packages, and printed circuit boards.

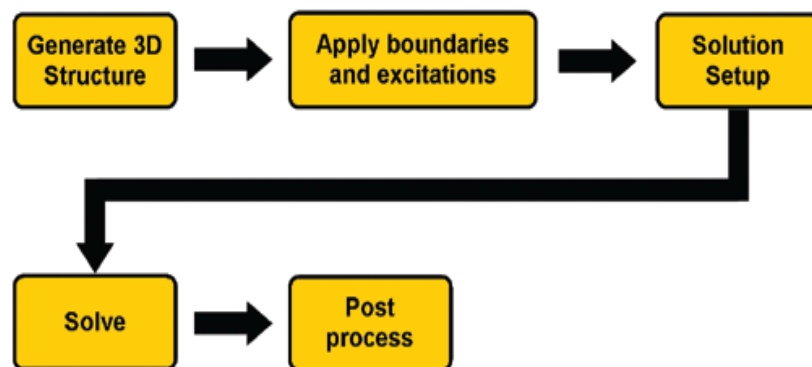


Figure 3.5 Design procedure

### 3.6 Design steps

When you first open Ansys HFSS Electronics Desktop, Figure 3.6 shows a screenshot.

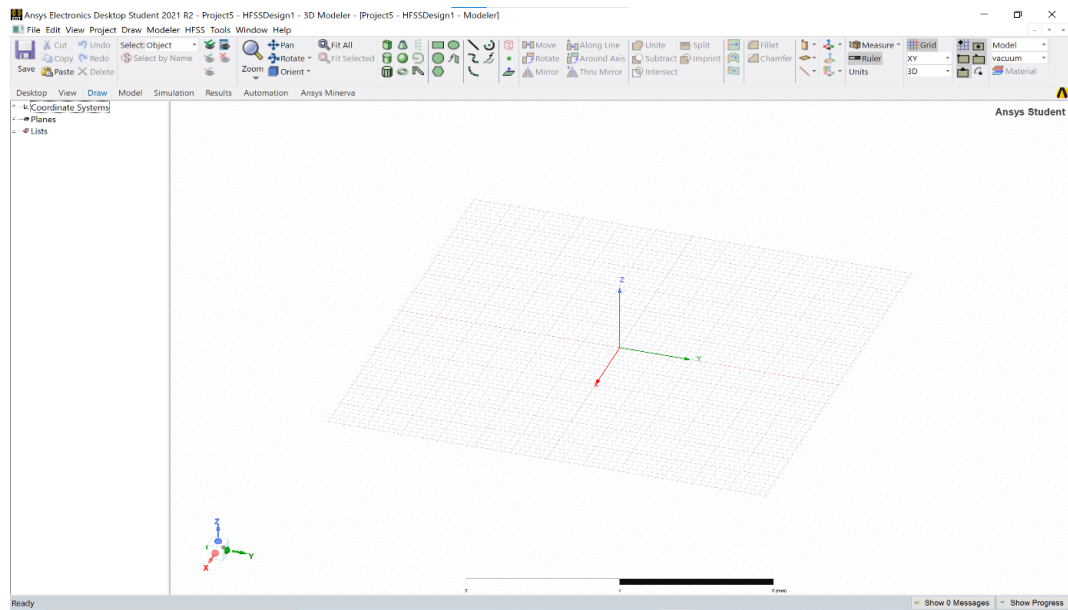


Figure 3.6 Screenshot of Ansys HFSS Electronics Desktop.

Then start drawing the first substrate and set the position, length, width, and height as shown in figure 3.7.

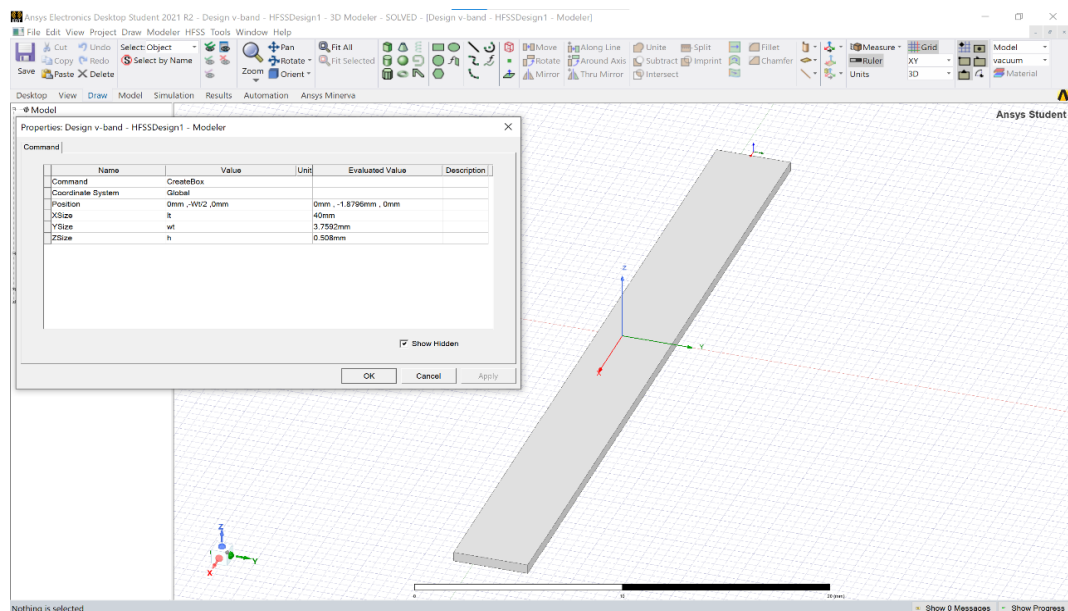


Figure 3.7 property design and the first substrate

As seen in figure 3.8, the same procedure as above starts with designing the second substrate with a z position higher than the first substrate and drawing and subtracting the AFSIW using a linear spline.

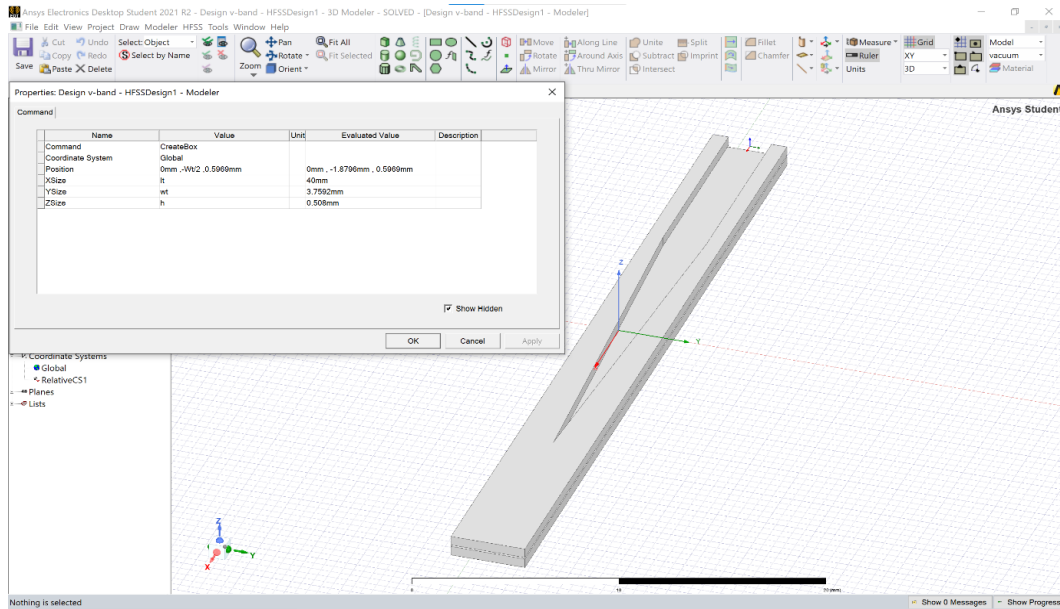


Figure 3.8 2<sup>nd</sup> substrate with a tapered shape

In the transition region, draw a linear spline with the dimensions shown in figure 9 with 9 points and two numbers of segments.

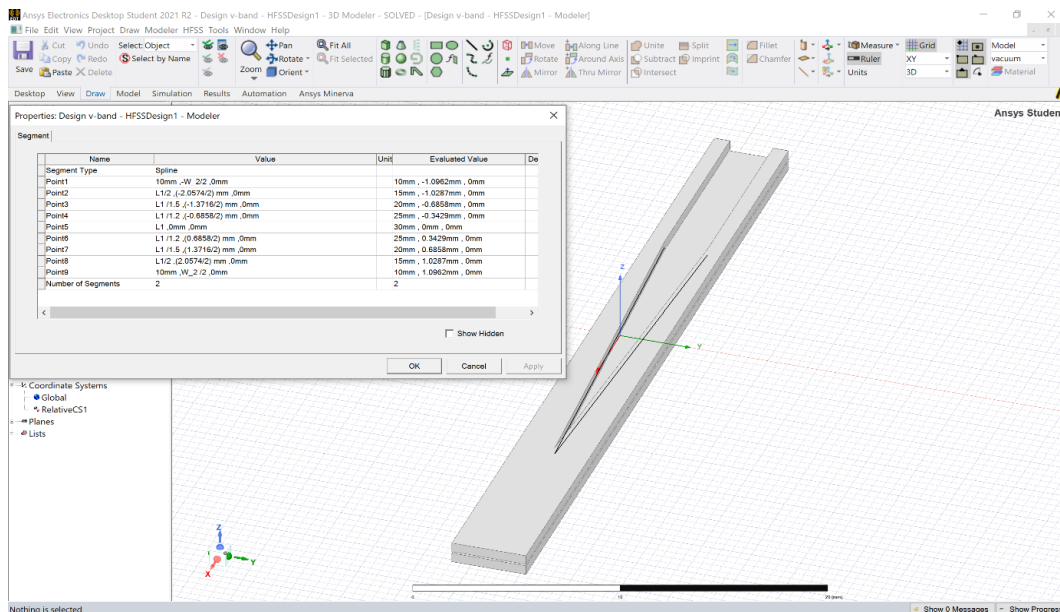


Figure 3.9 2<sup>nd</sup> substrate with tapered shape and properties

Then, as seen in figure 3.10, start drawing the rectangular hole on the second substrate on the one side and then use the mirror feature.

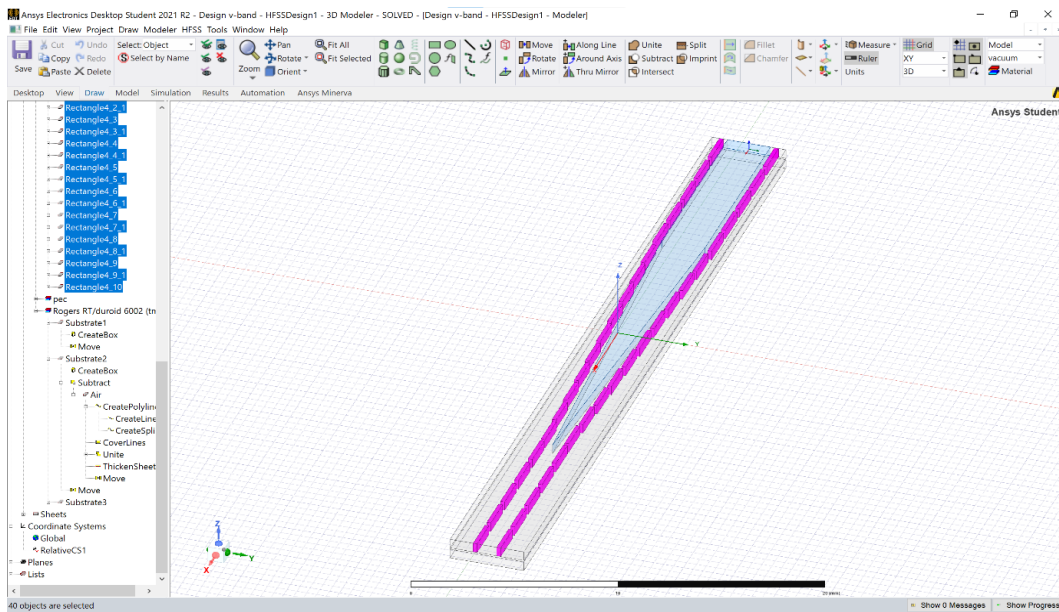


Figure 3.10 2<sup>nd</sup> substrate with a rectangular hole

Start by drawing the copper plates on all the faces with a 0.0889mm thickness, as shown in figure 3.11.

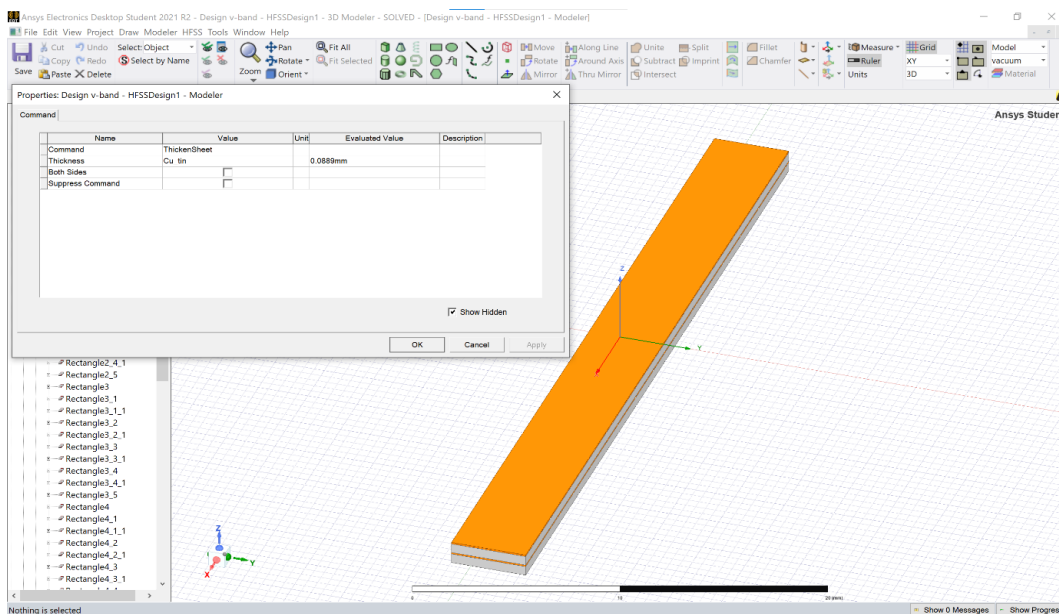


Figure 3.11 A copper plate and its properties

Figure 3.12 shows the completed three-dimensional design of the air-filled substrate integrated waveguide.

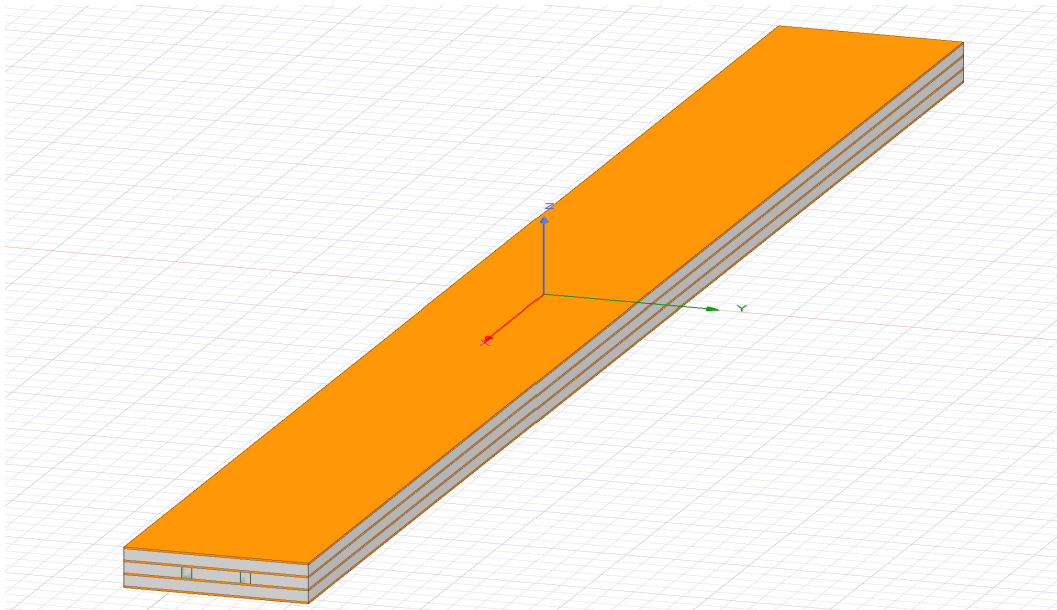


Figure 3.12 3D design of the AFSIW

Draw a box that encompasses the whole item, leaving about 1 mm or more on each design side. The location of the box, as well as its dimensions, may be seen in Figure 3.13 below.

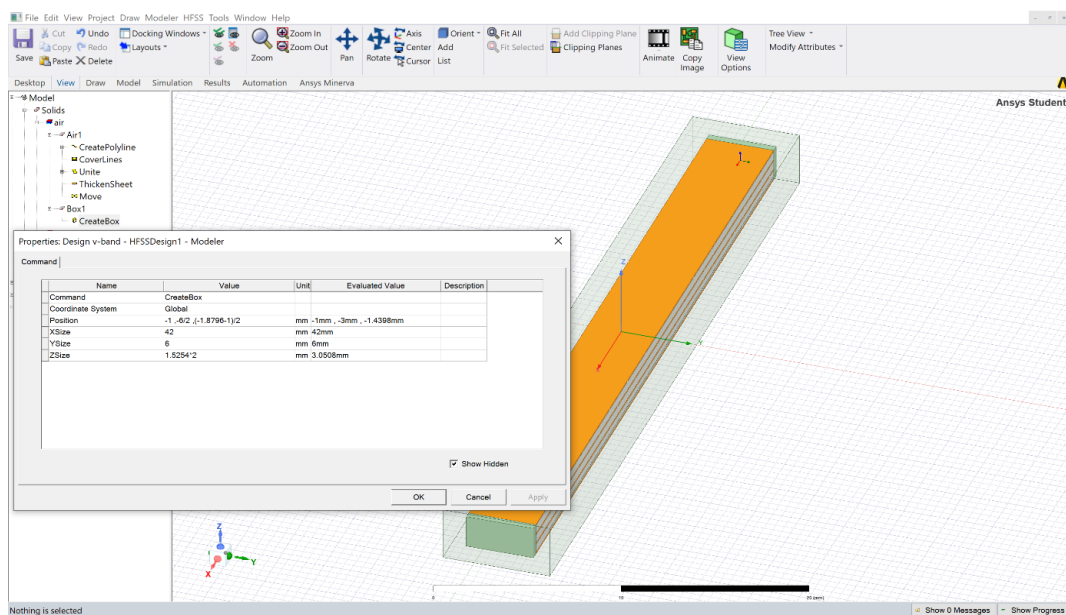


Figure 3.13 box and the characteristics of the box